International Journal of Bridge Engineering (IJBE), Vol. 9, No. 1 (2021), pp. 01-13

# OPTIMIZE ROBOTIC GMAW PARAMETERS FOR BUTT WELDING OF ALUMINUM 6061

Milad Bahrami [1], Michel Guillot [2]

[1,2] PI2/REGAL Research Team, Department of Mechanical Engineering, Laval University, Quebec, G1V 0A6, Canada
e-mail: milad.bahrami.1@ulaval.ca, michel.guillot@gmc.ulaval.ca

**ABSTRACT:** Metal Inert Gas (MIG) welding is a versatile gas metal arc welding (GMAW) process that uses a continuous solid wire electrode and a shielded gas to assemble both thin sheet and thick section components. As welding distortion and residual stress have negative effect on welding assembly, it is necessary to select the proper welding parameters. This study focuses on the optimization parameters for Metal Inert Gas (MIG) welding, Aluminum 6061 samples have been welded in V-groove butt joint configuration, with 60 degree angle and 6.35 mm thickness. Taguchi technique based Orthogonal Array (L4 and L8) is used for Design of Experiments (DOE) and artificial neural network (ANN) modeling is utilized to predict the distortion and Ultimate Tensile Strength (UTS). The 3d surface graphs and contour plots were generated for the results to elucidate the relationship between welding parameters, lack of penetration (LOP), ultimate tensile strength (UTS) and distortion. Afterward optimum process parameters are identified to maximize the UTS as well as minimize distortion and lack of penetration for the weld joint. The ideal range of process parameters such as voltage, wire feed speed, gun angle, distance between nozzle to weld, travel speed, root gap and root face have been found.

**KEYWORDS:** Distortion, Mechanical properties, Neural Modeling, Taguchi Method, Welding Parameters

## 1 INTRODUCTION

One of the main process for welding aluminum is gas metal arc welding (GMAW). Gas Metal Arc Welding (GMAW) is a process, which joins metals by heating the base and electrode metals to their melting point with an electric arc. The arc is between a continuous, consumable electrode wire and the metal being welded. The arc is shielded from contaminants in the atmosphere by a shielding gas [1]. Welding parameters have a strong effect in specifying the weld joint quality. GMAW involves many process parameters, such as arc current, workpiece thickness and welding geometry, wire electrode, feed rate, type of shielding gas, travel speed, gun angle, distance of the weld and nozzle, as well as

the alloys selected for the wire electrode and workpiece. Any of those parameters can influence the final quality of the welded products [2-6]

With the usage of the welding robot, production efficiency increased, the status of a welder changed and the stable welding quality required for automation was achieved [7]. There are several searches have been done in robot welding [8-14] but there is limit search about MIG welding on aluminum with robot.

There are many studies on the optimization of GMAW parameters for welding steel and aluminum [15-20]. Ibrahim et al [21] worked on the effects of welding speed on the robotic metal inert gas welding process and on the lack of penetration and microstructural properties of mild steel weldments of 6 mm plate. D. Bahar, et al [22] found the process parameters of MIG welding to optimize the hardness and ultimate tensile strength (UTS) by joining the dissimilar materials: mild steel (MS1020) and stainless steel (SS 316). Satyajitsinh et al [23] investigated on MIG welding process and also on Taguchi's Method. S. Kim et al. [24] found in their work that the optimization of a welding process involves finding the combination of parameters that can be shown as best vis-à-vis some standard and chosen parametric combination. Important welding parameters have been made as user-adjustable and the corresponding graphical interfaces have been provided for taking user inputs [26]. Jay Joshi et al [27] studied the effect of MIG welding parameters such as current, wire feed speed and gas flow using Grey Relational Analysis. ANOVA methodology used to analyze grey relational grade to find out the effect of each parameter. K.S.Pujari et al [28] optimized welding parameters of the weld pool geometry for AA 7075-T6 Aluminium alloy GTAW process.

In the present work, an experimentally study is conducted to optimized welding parameters on GMAW process. More specifically Al6061-T6 6.35 x 76.2 mm extrusions were butt welded using V grooves at 60 degrees. Experiments were performed by varying process parameters such as voltage(v), wire feed speed(WFS) and travel speed(TS), distance between weld and nozzle(DISW), root gap and root face. Taguchi method is used to design the experiments. Distortion, penetration and mechanical properties (UTS) were measured for all samples. After an artificial neural network (ANN) is created to predict and optimize the welding parameters on distortion, penetration and UTS. Finally, confirmation tests has been made to confirms the estimations of ANN models. For final test ultrasonic and liquid penetrant test were taken to evaluate surface defects on optimal samples.

## 2 EXPERIMENTAL PROCEDURE

### 2.1 Welding apparatus and material

In this study Fanuc R2000 robot and Miller Auto-Axcess 450 welding machine with pulsed arc welding technology are used to produce the welded samples. Figure 1 shows the process working of the robot.

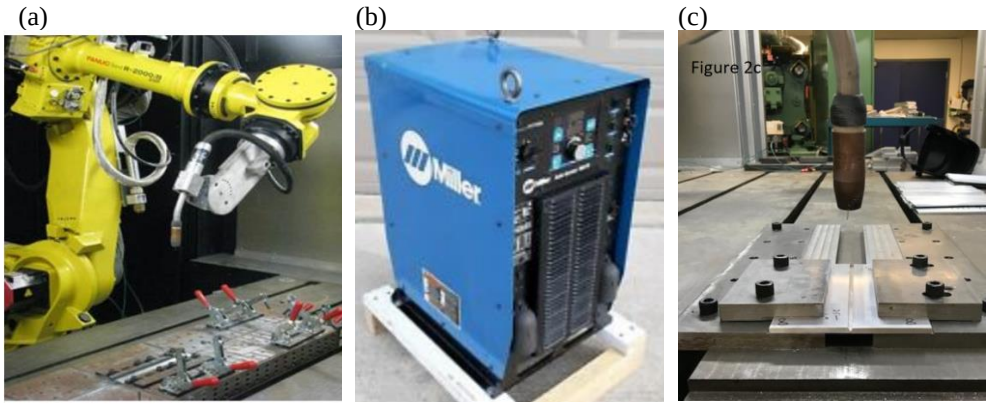


*Figure 1.* (a) Robot Fanuce R2000 (b) Miller Auto Axces 750 (c) Current welding process

Material Properties of base metal is the 6061-T6 aluminum has a nominal chemical composition of 0.99 wt% MG,0.58 wt% Si,20 wt% Cu, 0.35 wt% Fe, 0.12 wt% Cr, and 0.04 wt% Mn, and the rest is aluminum. Table 1 shows material properties of the aluminum 6061-T6.

*Table 1.* Chemical composition material and mechanical properties of aluminum 6061-T6

| | Chemical Composition (wt%) | | | | | | |
|---|---|---|---|---|---|---|---|
| Material | Al | Mg | Mn | Cu | Fe | Si | UTS (MPa) |
| AA-6061-T6 | Bal. | 0.83 | 0.07 | 0.19 | 0.19 | 0.55 | 285 |

Consumable, wire metal used for process is 5356 with 1.2 mm diameter, table 2 shows material properties of this wire, also 100% Argon used for gas protection with flow 0.71 cubic meters per hour (m3/hr) (25 cfh).

*Table 2.* Mechanical properties and chemical composition of wire 5356

| | Chemical Composition (wt%) | | | | | | | |
|---|---|---|---|---|---|---|---|---|
| Material | Al | Mg | Zn | Cu | Fe | Si | Other total | Shear moduls (GPa) |
| AA-6061-T6 | 92.9-95.3 | 4.5-5.5 | 0.1 | 0.10 | 0.4 | 0.25 | 0.15 | 26 |

In this study, extruded flat bars of aluminum 6061-T6 of size $245\ mm \times 88\ mm$ are supplied in the T6 condition. The butt welded V-Groove, 60 degree angle has been machined with different root face lengths. Different root gaps are set using calibrated shims, (Figure 2 geometry of joint).

(a) (b)

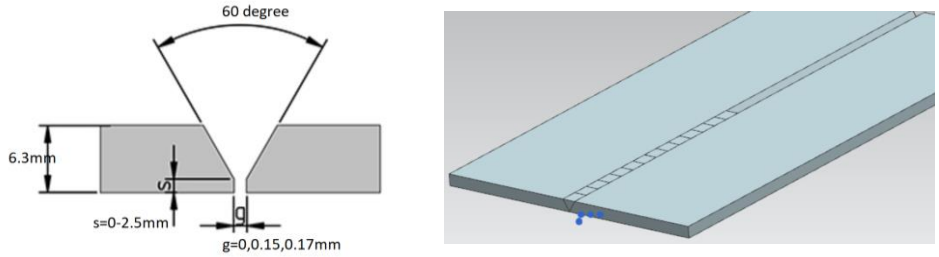


*Figure 2.* (a) Geometry of joint preparation (b) Geometry of the weld sample

## 2.2 Quality evaluation

**Non-destructive-test.** Ultrasonic test (UT) and liquid penetrant (LP) have been done for the confirmation test of the best results to validate the root penetration as well as the absence of surface defect. Reference standard for liquid penetrant of surface defects is CSA W 59.2. LP method used to check surface-breaking also find smallest crack or material not sealed by a weld for best samples. Ultrasonic test has been performed for best samples and there is no defect found. UT used to propagate into the metal and be reflected from surface scratches, voids, and other discontinuities. The ultrasonic test conforms to the requirements of the specifications ASTM E164, ultrasonic contact examination of weldments and ASME section V recommended practice for ultrasonic pulse-echo straight beam testing by contact method. The method of the pulse-echo is used as surface wave for detection of defects near the surface. Penetration has been verified by obtaining a reflection from an opposite parallel surface and also obtaining a back reflection on similar material while using approximately the same length of sound travel. The equipment for ultrasonic test is Olympus OmniScan MX and transducer details is 2.25 Mhz, 1/2 inch with 65 degree.

**Distortion.** Doing all welding on one side of a part will cause much more distortion than if the welds are alternated from one side to the other [28]. In this search distortion of the all plates has been measured by DEA Gamma 0101 coordinate measuring machine (CMM) with 40 points in the each plates (X-Y-Z), figure 3 shown schematic of distortion measurement. The method which is used to measure distortion by CMM is based on measuring a ball array. For all samples distortion has been measured using a Coordinate Measuring Machine. On the top surface of all sample, 40 points measured(X-Y-Z). The data has been analysed first by finding the best-fit plane which is used as a reference plane. Then the errors between the measured points and the reference plane were calculated as shown in figure 5.

(a) (b)

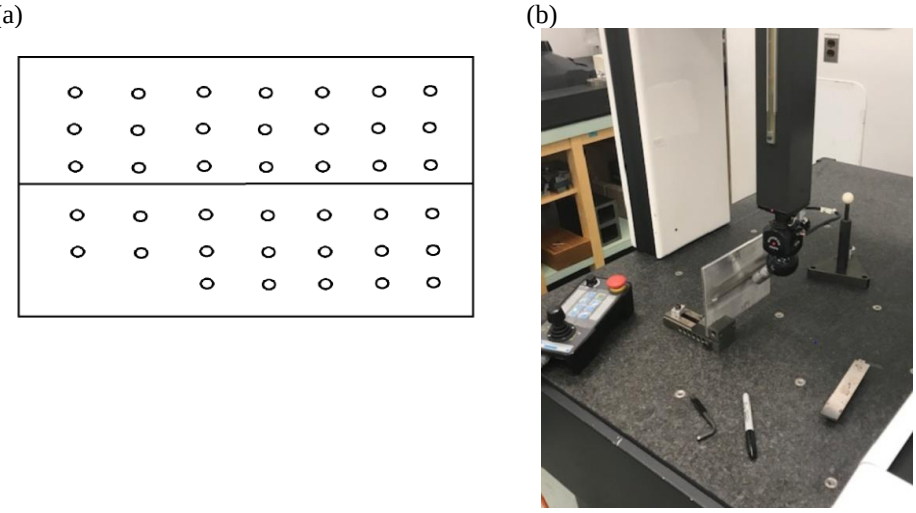

*Figure 3.* Distortion measurement (a) Position of 40 points on welded samples, (b) Current CMM machine for

**UTS.** To investigate the mechanical properties, tensile test of the weld joint were machined according to the American Society for Testing of Material (ASTM E8M-04) standard for all samples as shown figure 3a and 3b. Moreover, tensile tests were carried out at room temperature, after at least 7 days after welding operation. The equipment used for tensile test is a hydraulic testing machine employed with a load cell of 44.5 KN calibrated to 0.08kN under crosshead speed of 1 mm/min (Figure 3c).

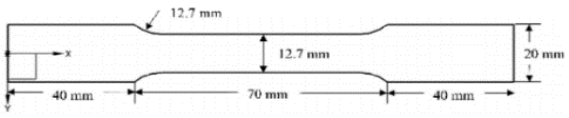


(a)

(b)

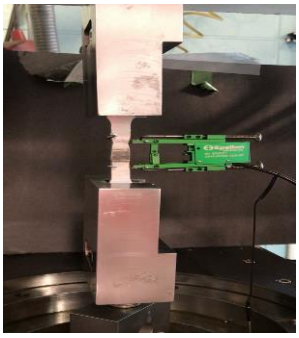

(c)

*Figure 4.* Force measurement process (a) Schematic of the sample for force, (b) Current samples for force measurement, (c) Press equipment for force measurement

**Lack of Penetration or incomplete penetration.** This type of defect is found in any of two ways of groove joint of weld: When the weld bead does not penetrate the entire thickness of the base plate. [29]. In this study the lack of penetration has been measured using a digital caliper and results indicated in mm. Note that for all samples with full penetration, the lack of penetration has been shown as zero mm.

## 3 EXPERIMENTAL PROCEDURE

### 3.1 Design of Experiments

In this search, the design of experiments (DOEs) apply various orthogonal arrays that are accumulated and used to train artificial neural network (ANN) model. In fact, the consequence of the welding parameters is investigated. First preliminary DOE had been carried out with three welding parameters and two level to find the preliminary results such as distortion, lack of penetration and UTS, and a (L4,L16) orthogonal array is used to explore the effect of the voltage(V), wire feed speed(WFS) and distance from nozzle to weld (DISW), and process parameters on the distortion, lack of penetration and UTS of the butt weld joints made by MIG technique. During this set of tests, different root gaps and different root faces were added. Results for UTS, voltage, distortion and Lack of penetration reviewed and evaluated for all tests (see Table 3). In table 3 the Travel speed is 10 mm/s and Gun angle is 11 degree.

### 3.2 Artificial neural network prediction model

An ANN was proposed to establish a relationship between output results and welding parameters. By using results from preliminary DOE, the first ANN model had been trained. In first ANN model, welding parameters are voltage, wire feed speed, distance between nozzle and weld, root faces and root gap. Table 4 shows the RMSE and Maximum error for the training and learning data for first ANN model. Table 5 shows the best parameters which respect to minimum distortion (less than 0.5 mm), minimum lack of penetration (less than 0.01 mm) and maximum UTS (more than 160 Mpa). Afterwards, based on acceptance levels of Table 4, a final DOE was designed to explore more around the optimal region identified by the ANN model. This DOE has been made of using Taguchi L8 with input parameters such as voltage, distance of the wire to sample, gun angle, root face, wire feed speed, gap between two plate and travel speed. Final DOE is L8 orthogonal array used to evaluate and find acceptable welding parameters. as well as four additional tests were made to find the best results (Table 6). By using final results from table 6, the second ANN model has been trained. To train the final ANN model, seven varying welding parameters have been selected.

*Table 3.* Preliminary design of experiments and error (DOE) with additional test

| | **Test nu.** | **V input (V output)** | **DISW (mm)** | **WFS (mm/s)** | **Root Gap (mm)** | **Root Face (mm)** | **Results 2 Lack of penetration (mm)** | **Results 3 Distortion (mm)** | **UTS (Mpa)** |
|---|---|---|---|---|---|---|---|---|---|
| Preliminary DOE | 1 | 55(19.2) | 12 | 63.5 | 0 | 2.5 | 2.75 | 1.2635 | 112 |
| | 2 | 55(20.4) | 10 | 84.66 | 0 | 2.5 | 1.16 | 0.3868 | 160 |
| | 3 | 65(22.8) | 12 | 84.66 | 0 | 2.5 | 2.1 | 0.3580 | 146 |
| | 4 | 65(21.5) | 10 | 63.5 | 0 | 2.5 | 2.63 | 0.5258 | 125 |
| Additional tests | 5 | 65(21.5) | 10 | 63.5 | 0.762 | 2.5 | 2.53 | 0.2377 | 118 |
| | 6 | 65(21.5) | 10 | 63.5 | 1.143 | 2.5 | 1.45 | 0.2800 | 126 |
| | 7 | 70(23.9) | 10 | 84.66 | 1.143 | 2.5 | 0 | 0.2686 | 207 |
| | 8 | 70(23.9) | 10 | 84.66 | 0.381 | 1.5 | 0 | 0.4067 | 208 |
| | 9A | 60(21.5) | 10 | 84.66 | 0 | 1.5 | 1.3 | 0.2807 | 132 |
| | 9B | 60(21.5) | 10 | 84.66 | 0 | 1.5 | 0 | 0.2807 | 210 |

*Table 4.* The RMSE and Maximum error for the training and learning data from first ANN

| **Distortion** | | | | **Lack of Penetration** | | | | **UTS** | | | |
|---|---|---|---|---|---|---|---|---|---|---|---|
| RMSE | | Max Error | | RMSE | | Max Error | | RMSE | | Max Error | |
| **Learned** | **Trained** | **Learned** | **Trained** | **Learned** | **Trained** | **Learned** | **Trained** | **Learned** | **Trained** | **Learned** | **Trained** |
| 5E-11 | 8E-11 | 4E-06 | 8E-06 | 3E-05 | 7E-05 | 0.0041 | 0.0078 | 0.062 | 0.17 | 0.33 | 0.77 |

*Table 5.* Acceptance parameters from first ANN

| **V** | **Travel speed** | **WFS** | **Gap** | **Root** | **Distortion(mm)** | **LOP(mm)** | **UTS** |
|---|---|---|---|---|---|---|---|
| 55-60 | 10 | 200 | 1-1.5 | 1.5 | 0.1-0.39 | 0 | 160-214 |
| 60-65 | 10 | 200 | 1-1.5 | 1.5-2.5 | | | |
| 70 | 10 | 200 | 0.5 | 2 | | | |

*Table 6.* Final L8 DOE with additional test

| | Test nu. | V input (volt) (voltage output) | WFS (mm/s) | TS (mm/s) | GA (Degree) | GAP (mm) | ROOT (mm) | DISW (mm) | Lack of penetration (mm) | Distortion (mm) | UTS (Mpa) |
|---|---|---|---|---|---|---|---|---|---|---|---|
| Final L8 DOE | 10 | 62(20.4) | 80.43 | 10 | 10 | 0 | 1.5 | 10 | 1.06 | 0.2807 | 130 |
| | 11 | 62(20.4) | 80.43 | 10 | 12 | 0.13 | 2.5 | 12 | 1.2 | 0.3336 | 132 |
| | 12 | 62(20.9) | 88.9 | 12 | 10 | 0 | 2.5 | 12 | 1.23 | 0.3600 | 131 |
| | 13 | 62(20.9) | 88.9 | 12 | 12 | 0.13 | 1.5 | 10 | 0 | 0.2878 | 181 |
| | 14 | 68(23.05) | 80.43 | 12 | 10 | 0.13 | 1.5 | 12 | 0 | 0.4328 | 202 |
| | 15 | 68(23.05) | 80.43 | 12 | 12 | 0 | 2.5 | 10 | 1.025 | 0.3930 | 178 |
| | 16 | 68(23.60) | 88.9 | 10 | 10 | 0.13 | 2.5 | 10 | 0 | 0.4235 | 202 |
| | 17 | 68(23.60) | 88.9 | 10 | 12 | 0 | 1.5 | 12 | 0 | 0.3320 | 209 |
| Additional tests | 18 | 66(22.90 | 84.66 | 11 | 11 | 0.07 | 2 | 11 | 0 | 0.5122 | 200 |
| | 19 | 70(23.90) | 88.9 | 11 | 11 | 0 | 2 | 11 | 0 | 0.3733 | 201 |
| | 20 | 70(23.70) | 84.66 | 10 | 10 | 0 | 2.5 | 10 | 0 | 0.4330 | 201 |
| | 21 | 69(23.5) | 88.9 | 10 | 10 | 0 | 2 | 10 | 0 | 0.5293 | 203 |

# 4 RESULTS AND DISCUSSION

## 4.1 Distortion

More specifically, figure 5(a) shows the error for worst sample (between -0.4 to +0.86 mm) and (b) for best sample (between -0.2 to +0.13 mm).

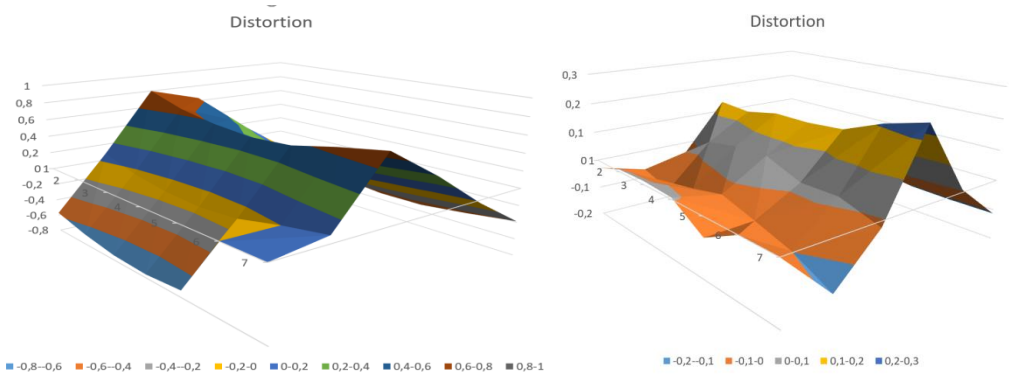


a. Test1.Average V error 1.263567283 mm b. Test5.Average V error 0. 2377045 mm

*Figure 5.* (a) Errors in sample 1 having maximum distortion (b) Errors in sample 5 having minimum distortion

From the ANN model of distortion trained with experimental data of table 6, the graphs it was found have been evaluated and results for distortion less than 0.5 mm were accepted, figure 6a shows 3d contour plot of distortion for three different voltage, in this figure horizontal axes is wire feed speed(WFS) and vertical axes is travel speed(TS).

## 4.2 Lack of penetration

Results of analyse from ANN has been evaluated and results for lack of penetration less than 0.01 mm were accepted. This amount which means there is a full penetration for welding joint. Figure 6b shows 3d contour plot for lack of penetration for three different voltage. In these figure horizontal axes is wire feed speed (WFS) and vertical axes is travel speed (TS). Results help to find optimization parameters.

## 4.3 UTS

Results of analyse the data from ANN has been evaluated and results for UTS more than 160 Mpa were accepted. Figure 6c shows some examples of 3d contour plot for UTS on three different voltage. In these figure horizontal axes is wire feed speed (WFS) and vertical axes is travel speed (TS).

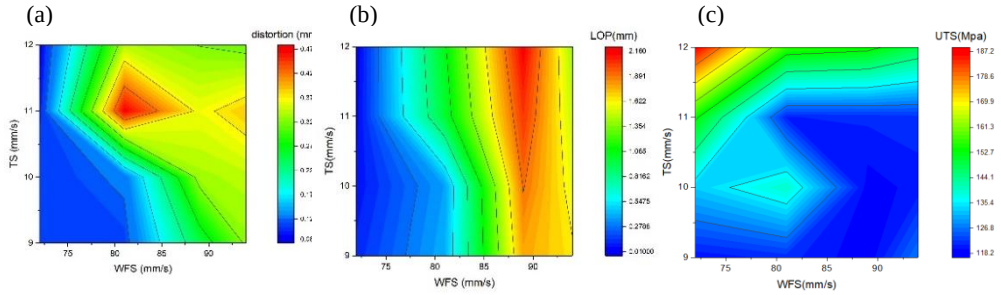


*(1) V=19v.WFS=72-94mm/s.TS=9-12mm/s.GA=11degree. GAP=0.125mm. Root Face=2.5mm.DISW=10mm*

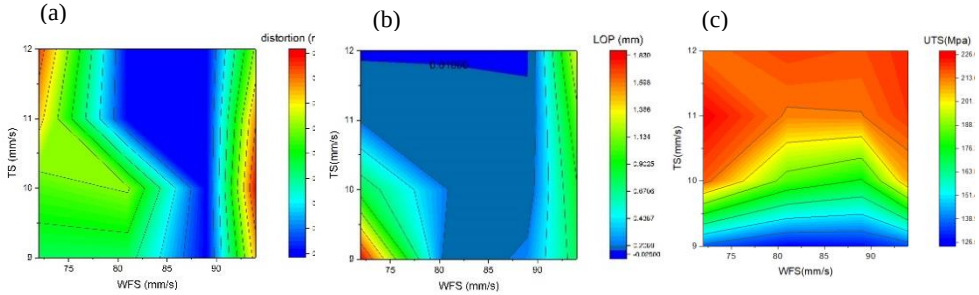


*(2) V=23v.WFS=73-94mm/s.TS=9-12mm/s.GA=12degree. GAP=0.125mm. Root Face=2mm.DISW=10mm*

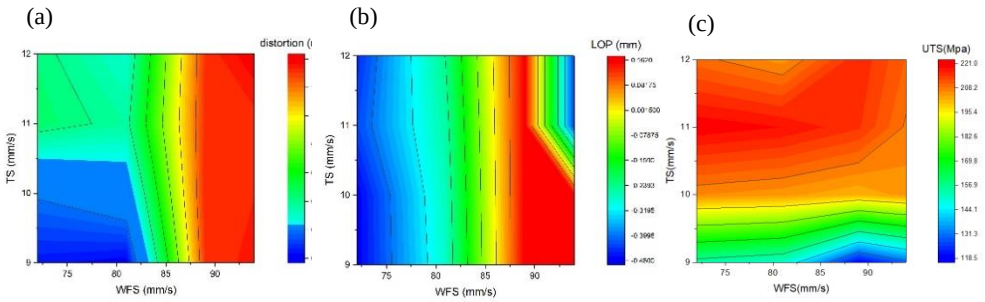


*(3) V=24.5v.WFS=81-94 mm/s.TS=9-12mm/s.GA=11degree. GAP=0.17mm. Root Face=2.5mm.DISW=9mm*

*Figure 6.* Contour plot of the (a) Distortion less than 0.5mm is acceptable range) (b) Lack of penetration less than 0.01mm is acceptable range)(c)UTS more than 160 Mpa is acceptable range). with wire feed speed and travel speed with different other parameters

The reason to choose WFS/TS is, after analyse entire data, the only voltage have been found for acceptance results of distortion, lack of penetration and UTS is 19, 23 and 24.5v.

## 5 MODEL VALIDATION AND CONFIRMATION TEST

### 5.1 Optimization of welding process

To find optimized welding parameters, more analyses has been done from all ANN model data, and acceptance data for distortion (less than 0.5 mm), lack of penetration (less than 0.01) and UTS (over 160 Mpa) has been investigated and the intersection of three sets of results have been found as an optimized parameters, table 8 has been shown optimized parameters with results for butt welds joint on Aluminum6061. Table 7 shows the RMSE and Maximum error for the training and learning data for combination of DOEs.

*Table 7.* The RMSE and Maximum error for the training and learning data from combination both DOE for 21 tests

| **Distortion** | | | | **Lack of Penetration** | | | | **UTS** | | | |
|---|---|---|---|---|---|---|---|---|---|---|---|
| RMSE | | Max Error | | RMSE | | Max Error | | RMSE | | Max Error | |
| **Learned** | **Trained** | **Learned** | **Trained** | **Learned** | **Trained** | **Learned** | **Trained** | **Learned** | **Trained** | **Learned** | **Trained** |
| 9 E-009 | 8E-005 | 3E-005 | 0.004 | 0.84 | 0.82 | 0.63 | 0.61 | 0.0004 | 0.00038 | 0.004 | 0.005 |

*Table 8.* Optimized parameters with acceptance results

| **V** | **WFS** | **TS** | **GA** | **GAP** | **Root Face** | **DistW** | **Distortion** | **Lack of Penetration** | **UTS** |
|---|---|---|---|---|---|---|---|---|---|
| 19 | 72 | 12 | 11 | 0-0.17 | 2 | 10-11 | 0.01-0.49 | 0 | 167-235 |
| 23 | 72-94 | 11-12 | 10-12 | 0-0.17 | 2-2.5 | 9-11 | | | |
| 24.5 | 81-94 | 9-12 | 9-11 | 0-0.17 | 2.5 | 9-11 | | | |

## 5.2 Confirmation tests

Afterwards, based on results of developed ANN models (Table 8), a final set of tests have been welded and the results of the best parameters have been found and shown in table 8, for confirmation tests, liquid penetrant and ultrasonic test have been performed and results are shown in table9. (Test 25 to 28 are repeatability of the optimized parameters)

*Table 9.* Confirmation tests

| | **Test nu.** | **Voltage** | **WFS** | **TS** | **GA** | **Root Gap** | **Root Face** | **DISW** | **LOP** | **Distortion** | **UTS** | **NDT** |
|---|---|---|---|---|---|---|---|---|---|---|---|---|
| | | | **mm/s** | **mm/s** | **degree** | **mm** | **mm** | **mm** | **mm** | **mm** | **Mpa** | **Pass/ Fail** |
| Confirmation test | 22 | 25 | 93 | 11 | 10 | 0 | 2 | 10 | 1.02 | 0.9 | 137 | Fail |
| | 23 | 24.2 | 93 | 11 | 10 | 0 | 2 | 10 | 0 | 0.5 | 191 | Pass |
| | 24 | 23.7 | 89 | 12 | 10 | 0.125 | 2 | 10 | 0 | 0.9 | 165 | Pass |
| | 25 | 24.5 | 93 | 12 | 10 | 0.125 | 2.5 | 10 | 0 | 0.33 | 203 | Pass |
| Repeatability Tests | 26 | 24.5 | 93 | 12 | 10 | 0.125 | 2.5 | 10 | 0 | 0.41 | 203 | Pass |
| | 27 | 24.5 | 93 | 12 | 10 | 0.125 | 2.5 | 10 | 0 | 0.33 | 207 | Pass |
| | 28 | 24.5 | 93 | 12 | 10 | 0.125 | 2.5 | 10 | 0 | 0.35 | 200 | Pass |

## 6 CONCLUSIONS

Parameter optimization based on the experimental samples and ANN models has been presented in this paper. In this study. Gas Metal Arc Welding is used to weld the two similar aluminium alloys. the number of welding tests is finalized in the experimental process by Taguchi method. The results of this study can be summarized as follows:

- The effect of parameters and the best working window providing maximum UTS with minimum distortion and zero lack of penetration on butt welding of AA6061-T6 has been established for MIG welding
- For all UTS more than 160 Mpa, full penetration was accomplished
- For one pass welds of the butt weld joint 6.35 mm plate and also using ANN, it was found that voltage, wire feed speed and travel speed are the most influencing parameter on the quality of the weldments, distortion, lack of penetration and UTS.
- Based on the tensile properties. distortion and lack of penetration results, the optimum welding parameters is 24.5v, wire feed speed 93 mm/s, travel speed 12 mm/s, gun angle 10 degree.

## Author Contributions:

**Funding:** This research has been supported by funds of PI[2] Team.
**Conflicts of Interest:** The authors declare no conflict of interest.

## REFERENCES

[1] Anders. A. (2003). "Tracking down the origin of arc plasma science-II. Early continuous discharges." IEEE Transactions on Plasma Science. 31 (5): 1060–9.
[2] Fiona F. Chen et al. Model-based parameter optimization for arc welding process simulation. Applied Mathematical Modelling journal. 81 (2020) 386–400
[3] K. Weman. Welding Processes Handbook. Woodhead. Cambridge. 2003
[4] K. Weman and G. Lindén (eds). MIG Welding Guide. Woodhead Publishing 2006
[5] P. Bengtsson. Increasing productivity of metal-active-gas welding. it is possible. Der Praktiker 45 (8) (1993) 428–430
[6] M.H. Cho. D.F. Farson. Understanding bead hump formation in gas metal arc welding using a numerical simulation. Metall. Mater. Trans. B: Process Metall. Mater. Process. Sci. 38 (2007) 305–319
[7] S. Yumurtacı. T. Mert. TMMOB: Engineers & Machineries. 50. (2009)
[8] N.B.Landg et al, "Tensile Strength Analysis of V Groove Butt Weld Joint For Aluminum Alloys Aa 2025 & Aa 7025", IJARIIE-ISSN(O)-2395-4396, Vol-2 Issue-6 2019
[9] Kaoru Yoshikawa. Kazuo TanakaWelding robots for steel frame structures. Comput Civ Infrastruct Eng. 12 (1) (2002). pp. 43-56)
[10] Masahiro Nagata. Norimitsu Baba. Hiroshi Tachikawa. Steel frame welding robot systems and their application at the construction site Microcom Civ Eng (12) (1997). pp. 15-30
[11] Zhu Zhiming. N.I. Zhen. M.A. Guorui. Rail type all-position welding robot for box-type steel structures. China: CN103286494 B [P] (2015)
[12] Zhu Zhiming. M.A. Guorui. L.iu Han. The structure design of box-type steel structure welding robot Welding & Joining (3) (2014). pp. 2-7
[13] Robotic Welding Technology TS Hong and M Ghobakhloo. Universiti Putra Malaysia. Selangor. Malaysia W Khaksar. University Tenaga Nasional. Selangor. Malaysia.
[14] Zhou Jianru. Zhao XifangVibration analysis of Shanghai I robot [J] Noise and vibration control. 1 (1995). pp. 28-30.
[15] Campbell SW, Galloway AM, and McPherson NA. Artificial neural network prediction of weld geometry performed using GMAW with alternating shielding gases. Weld J 2012; 91(6): 174s-181s..
[16] S. Pal. S.K. Malviya. S.K. Pal. A.K. Samantaray, International Journal Advanced Manufacturing Technology. Vol. 44. 2009. pp.1250–1260
[17] R.V. Rao. V.D. Kalyankar. G. Waghmare. Applied Mathematical Modelling. Vol. 38 . 2014. pp. 5592–5608
[18] Chokkalingham S, Chandrasekhar N, and Vasudevan M. Predicting the depth of penetration and weld bead width from the infra red thermal image of the weld pool using artificial neural network modeling. J Intell Manuf 2012; 23(5): 1995-2001.
[19] J.P. Ganjigatti. D.K. Pratihar. A.R. Choudhury. Journal Material Process Technology. Vol. 189. 2007. pp. 352–366
[20] N. Murugan and R.S. Parmar. Journal of Materials Processing Technology. Vol. 41. 1994. pp. 381-398
[21] I.A. Ibrahim. S.A. Mohamat. A. Amir. A. Ghalib. Procedia Engineering 41. 2012. pp. 1502 – 1506.
[22] D. Bahar. Md Nawaz Sharif. K. Shravan Kumar. D. Reddy. Optimization of MIGwelding process parameters for hardness and strength of welding joint usingGrey relational analysis. Int. J. Res. Adv. Technol. 6 (5) (2018). E-ISSN: 2321-963.
[23] Satyajitsinh P. Chavda. A review on optimization of MIG welding parameters using Taguchi

DOE method. Int. J.Eng. Manage. Res. 4 (1) (2014). ISSN No.: 2250-075
[24] S. Kim. S.H. Lee. P.K.D.V. Yarlagadda. Comparison of multiple regression andback propagation neural network approaches in modelling top bead height ofmultipass gas metal arc welds. Sci. Technol. Weld. Joining 8 (5) (2003) 347–352
[25] JunXiong. Shuangyang Zou. Active vision sensing and feedback control of back penetration for thin sheet aluminum alloy in pulsed MIG suspension welding. Journal of Process Control Volume 77. May 2019. Pages 89-96.
[26] IIW Document 212-1634-19. 72nd IIW Annual Assembly and International Conference. Bratislava. Slovakia 2019
[27] Jay Joshi. Manthan Thakkar. Sahil VoraParametric optimization of metal inert gas welding and tungsten inert gas welding by using analysis of variance and grey relational analysis Int. J. Sci. Res. (IJSR). 3 (6) (2014). pp. 1099-1103 ISSN 2319–7064
[28] K.S.Pujari. . D.V.Patil. Gurunath Mewundi. Selection of GTAW process parameter and optimizing the weld pool geometry for AA 7075-T6 Aluminium alloy. Materials Today: Proceedings Volume 5. Issue 11. Part 3. 2018. Pages 25045-25055
[29] Welding Mig Hand book. Welding defect. Lack of penetration Esabna work company. 592mig10-2